

Generation and Reactivity of a $\text{Ni}^{\text{III}}_2(\mu\text{-}1,2\text{-peroxo})$ Complex

Norman Zhao, Alexander S. Filatov, Jiaze Xie, Ethan A. Hill, and John S. Anderson*

Department of Chemistry, University of Chicago, Chicago, Illinois 60637, United States

Supporting Information Placeholder

ABSTRACT: Ni-based oxide materials are promising candidates for catalyzing the oxygen evolution reaction. The detailed mechanism of water splitting in these systems has been of interest with a goal of understanding the intermediate species vital for catalytic activity. A potential intermediate species prior to release of oxygen is a bridging $\text{Ni}^{\text{III}}_2(\mu\text{-}1,2\text{-peroxo})$ complex. However, $\text{Ni}_2(\mu\text{-}1,2\text{-peroxo})$ complexes are rare in general and are unknown with oxidation states higher than Ni^{II} . Herein, we report the isolation of such an unusual high-valent species in a $\text{Ni}^{\text{III}}_2(\mu\text{-}1,2\text{-peroxo})$ complex, which has been characterized using single-crystal X-ray diffraction and X-ray absorption, NMR, and UV-vis spectroscopies. In addition, treatment with excess tetrabutylammonium chloride results in regeneration of the precursor Ni-Cl species, implicating the reversible release of oxygen or a reactive oxygen species. Taken together, this suggests that $\text{Ni}^{\text{III}}_2(\mu\text{-}1,2\text{-peroxo})$ species are accessible and may be viable intermediates during the oxygen evolution reaction.

The availability of cost-effective and abundant energy storage methods remains a significant challenge to effectively harnessing solar energy.¹ Electrochemical or photochemical water splitting to form oxygen and hydrogen presents a scalable option for the storage of solar energy in the form of chemical bonds, but most catalysts developed for hydrogen and oxygen evolution employ precious metals such as Ir and Pt, hindering large-scale use. For this reason, water splitting catalysts using first-row transition metals have become a desirable alternative.² Recently, Ni-based layered double hydroxides (LDH) have shown great promise due to their stability and high catalytic activity.^{3–6}

Given the properties of LDH materials, studies have been aimed at understanding their mechanism and function. While Ni-only LDH materials display oxygen evolution reactivity, superior catalysts are generated with incorporation of other transition metals such as Fe.^{7–9} Of particular interest in [NiFe]-LDH materials is to determine whether Ni or Fe is the active site for oxygen evolution.^{10–17} While Fe active sites have been proposed due to the higher turnover frequencies of [NiFe]-LDH materials, Ni remains an essential component of the most active catalysts. In these and other synthetic systems high-valent peroxo species, potentially arising from oxo-oxo coupling, are key proposed intermediates prior to oxygen release.^{18,19}

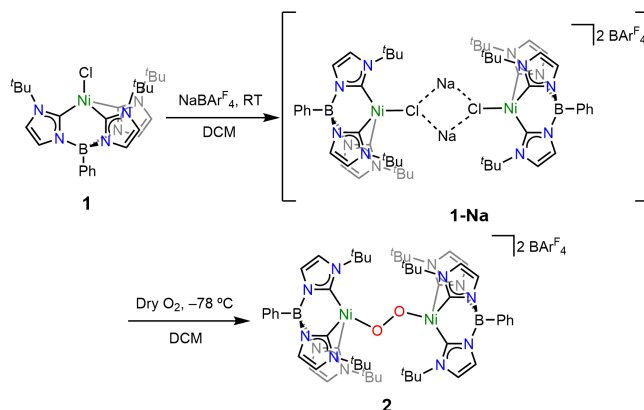
While there have been increasing examples of systems with high valent ($>2+$) Ni centers,^{20–23} this area is underdeveloped with regard to structurally characterized oxygen-containing intermediates that may have relevance to oxygen evolution. While examples of bimetallic dioxygen complexes of iron,

copper, and cobalt have been isolated and studied,^{24–31} only a handful of Ni-dioxygen complexes have been isolated such as bis- $\mu\text{-oxo}$ and bis- $\mu\text{-superoxo}$ species.^{32–38} Some binuclear $\text{Ni}^{\text{II}}(\mu\text{-}1,2\text{-peroxo})$ complexes have been transiently observed,^{39,40} but only one example has been structurally characterized.⁴¹ As such, the viability of high-valent Ni-peroxo intermediates remains unknown.

Previously, the tris(NHC)phenylborate (NHC = N-heterocyclic carbene) ligand $\text{PhB}(\text{tBuIm})_3^-$ has been used to stabilize unusual high-valent $\text{Co}^{\text{III}}\text{-oxo}$ and $\text{Fe}^{\text{IV,V}}\text{-nitride}$ complexes.^{42–44} We rationalized that this system might also aid in the stabilization and characterization of high-valent Ni complexes with oxygen-based ligands. Herein, we report the use of $\text{PhB}(\text{tBuIm})_3^-$ to isolate the first example of a $\text{Ni}^{\text{III}}_2(\mu\text{-}1,2\text{-peroxo})$ complex $\{[\text{PhB}(\text{tBuIm})_3]\text{Ni}-\text{O}-\text{Ni}[(\text{tBuIm})_3\text{BPh}]\}\{\text{BAR}^{\text{F}}_4\}_2$ (**2**, $\text{BAR}^{\text{F}}_4 = \text{tetrakis}(3,5\text{-bis}(\text{trifluoromethyl})\text{phenyl})\text{borate}$). Complex **2** has been structurally characterized, and its properties examined using a variety of techniques including ^1H NMR, UV-vis, and X-ray absorption spectroscopies. Furthermore, addition of simple nucleophiles such as Cl^- has been shown to regenerate the starting terminal chloride complex, suggesting the release of oxygen or reactive oxygen species. These results demonstrate that high-valent Ni-peroxo intermediates are indeed synthetically accessible and may be viable intermediates in oxygen evolution.

The synthesis of the Ni-chloride precursor $[\text{PhB}(\text{tBuIm})_3]\text{NiCl}$ (**1**) was recently reported by our group.⁴⁵ As **1** shows no reactivity under an atmosphere of oxygen for several days, we screened common halide abstractors such as Na^+ , Ag^+ , and Tl^+ salts to encourage reactivity. While Ag^+ or Tl^+ led to no tractable reactivity, treatment of **1** with $\text{NaBAR}^{\text{F}}_4$ in dichloromethane (DCM) causes the solution to change from a

Scheme 1. Synthesis of **1-Na** and **2**.



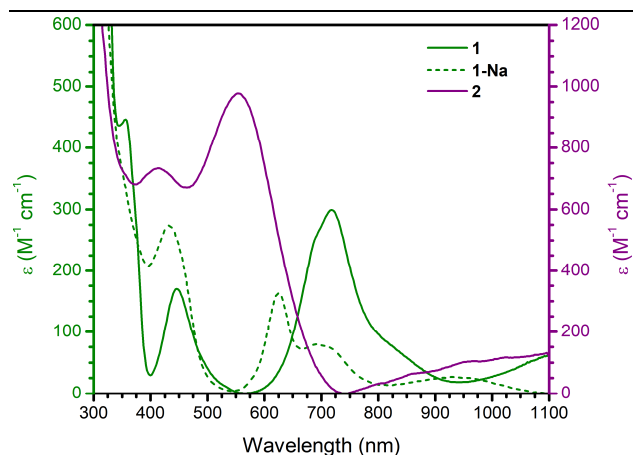


Figure 1. UV-vis spectra of **1**, **1-Na** (at RT) and **2** (at $-78\text{ }^{\circ}\text{C}$) in DCM. Left y-axis is for **1** and **1-Na**, and right y-axis is for **2**.

dull chartreuse green to an intense emerald green, indicative of the formation of a new species **1-Na** (Scheme 1). We found that a similar color change is observed in other non-coordinating solvents such as 1,3-difluorobenzene. However, **1-Na** is extremely sensitive to even small amounts of coordinating impurities such as ethers or variation in preparation conditions precluding detailed characterization of this species (Figure S1). While we do not have concrete characterization data on this complex, we tentatively propose an intermediate structurally similar to **1** with a weak interaction between the Na^+ ion and the chloride ligand. The proposed similar structure is also supported by comparing the paramagnetic ^1H NMR spectra of **1** and **1-Na** that show a shifted, but similar overall pattern of resonances. Furthermore, treatment of **1-Na** with 12-crown-4 ether to sequester Na^+ ions regenerates **1** by ^1H NMR spectroscopy (Figure S2). Based on these data, and similar species previously reported, we tentatively propose that **1-Na** is a dimer as depicted in Scheme 1.⁴⁶

Treatment of **1-Na** in DCM with dry oxygen at room temperature results in an intractable brown mixture of diamagnetic products as ascertained by ^1H NMR spectroscopy. However, at $-78\text{ }^{\circ}\text{C}$ addition of dry oxygen to **1-Na** in DCM results in a color change from emerald green to dark purple. We assign this new purple species as a dimeric $\text{Ni}^{\text{III}}_2(\mu\text{-}1,2\text{-peroxo})$ complex $\{[\text{PhB}(\text{tBuIm})_3]\text{Ni-O-O-Ni}[(\text{tBuIm})_3\text{BPh}]\}\{\text{BARF}_4\}_2$, **2** (Scheme 1). The distinct color change is reflected in the low temperature UV-vis spectrum of **2** (Figure 1) displaying features at 410 nm ($740\text{ M}^{-1}\text{cm}^{-1}$) and 550 nm ($970\text{ M}^{-1}\text{cm}^{-1}$) which are dramatically different from those in **1** or **1-Na**. Monitoring the oxygen addition reaction by UV-vis spectroscopy at low-temperature showed complete consumption of the starting material nearly instantaneously upon addition of O_2 at $-78\text{ }^{\circ}\text{C}$ (Figure S3). The extremely fast rate of this reaction combined with the sensitivity of **1-Na** precluded a more detailed examination of the solution dynamics of the oxygenation reaction.

Fortunately, dark purple crystals of **2** can be grown from concentrated DCM over several days at $-78\text{ }^{\circ}\text{C}$. Single crystal X-ray diffraction (SXR) confirms the formation of a $\text{Ni}^{\text{III}}_2(\mu\text{-}1,2\text{-peroxo})$ complex **2** (Figure 2). While the quality of the dataset is limited due to large numbers of solvent molecules and severe disorder of BARF_4 counterions, the atomic connectivity of **2** can be concretely ascertained. The O–O bond length in **2** is $1.40(1)\text{ \AA}$. This is shorter than the $1.465(2)\text{ \AA}$ observed

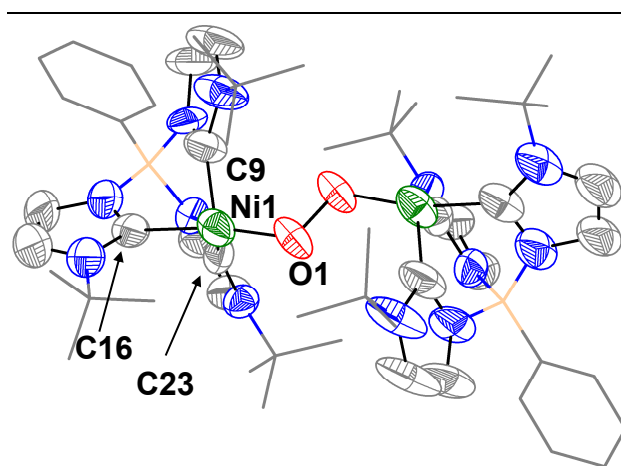


Figure 2. SXR structure of **2**. Ni shown in green, oxygen in red, carbon in grey, nitrogen in blue and boron in tan. Ellipsoids are shown at 50% probability. Solvent molecules, counterions and H-atoms omitted and parts of ligand scaffold shown as wireframe for clarity.

in a recent example of a $\text{Ni}^{\text{II}}_2(\mu\text{-}1,2\text{-peroxo})$ complex supported by a β -diketiminate scaffold.⁴¹ For comparison, the O–O bond length in hydrogen peroxide is 1.49 \AA and $\mu\text{-}1,2\text{-peroxo}$ complexes of Co have displayed O–O bond lengths that range from 1.34 to 1.49 \AA .⁴⁷ Meanwhile, the O–O bond lengths in two previously isolated $\text{Ni}_2(\mu\text{-}1,2\text{-superoxo})$ complexes are 1.33 and 1.35 \AA .^{33,41} The solid-state structure of **2** shows that the Ni^{III} centers adopt a seesaw geometry, with a Ni–O bond length of $1.79(1)\text{ \AA}$ and a Ni–O–O–Ni dihedral angle of $161.8(5)^{\circ}$. The Ni–O bond lengths are shorter than those of the recently isolated $\text{Ni}^{\text{II}}_2(\mu\text{-}1,2\text{-peroxo})$ complex, which has Ni–O bond lengths of $1.834(2)\text{ \AA}$ and a dihedral angle of $89.9(2)^{\circ}$.⁴¹ The shorter Ni–O distances are consistent with a higher oxidation state of Ni^{III} in **2**.

A similar solution and solid-state structure of **2** is supported by NMR data. The ^1H NMR spectrum of **2** collected at $-78\text{ }^{\circ}\text{C}$ has broadened and shifted resonances, consistent with a paramagnetic species (Figure S4). In compound **1**, the ^1H NMR resonances at 106 and 16 ppm have been assigned to the hydrogens of the imidazol-2-ylidene backbone. A similar pattern is seen in **2**, but with a doubling of these signals (109, 100, -13 , -15 ppm), which suggests the presence of an asymmetric dimer at $-78\text{ }^{\circ}\text{C}$. We propose this pattern arises from a combination of the seesaw geometry about the Ni centers and dynamics about the B–Ni–O vector at $-78\text{ }^{\circ}\text{C}$, as previously observed in a terminal Ni methyl complex supported by this tris(NHC) ligand scaffold.⁴⁵ The same ^1H NMR spectra are observed for samples of crystalline **2** dissolved in $\text{d}_2\text{-DCM}$ and samples of **2** generated *in situ* by addition of O_2 to **1-Na**, confirming that complex **2** is formed *in situ* in a relatively clean manner.

The effective magnetic moment of **2** was measured by Evans' method at $-78\text{ }^{\circ}\text{C}$ to be $\mu_{\text{eff}} = 3.35(7)\mu_{\text{B}}$. This value is potentially consistent with either ferromagnetic coupling between two $S = 1/2$ Ni^{III} centers ($\mu_{\text{S.O.}} = 2.82\mu_{\text{B}}$) or weak coupling between these centers ($\mu_{\text{S.O.}} = 2.45\mu_{\text{B}}$). Additionally, the X-band electron paramagnetic resonance (EPR) spectrum of a solution of **2** in DCM at 15 K is nearly silent, with only a weak signal centered around $g = 2$ accounting for less than 10% of the Ni in the sample. While metal complexes bridged by dioxygen ligands are commonly antiferromagnetically coupled,

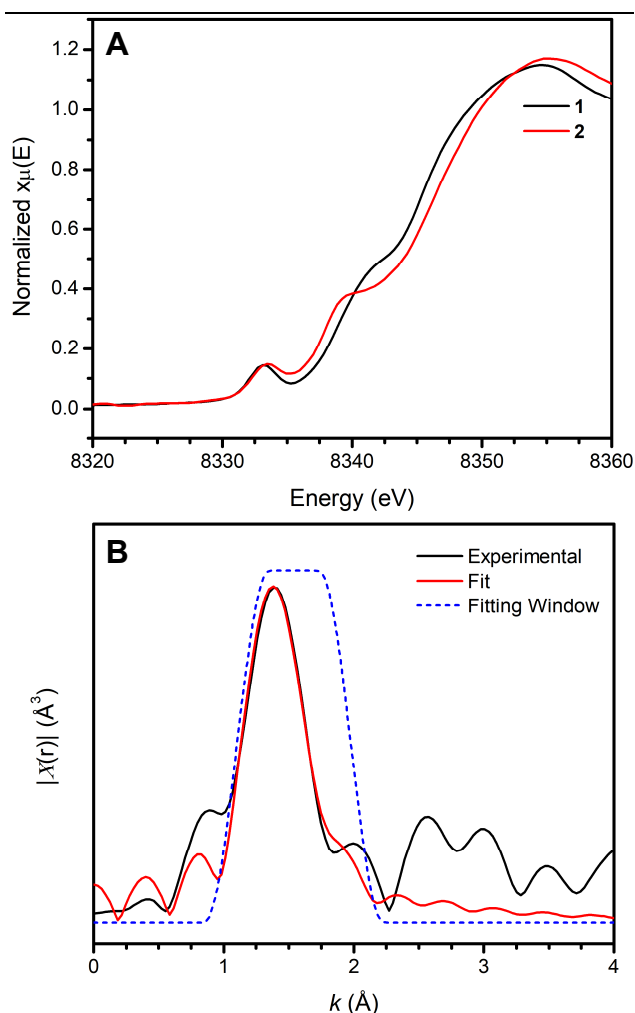


Figure 3. (A) Ni K-edge X-ray absorption of **1** and **2**, showing the normalized energies of the XANES region. (B) EXAFS spectrum (black) and fit (red) in R-space at the Ni K-edge absorption of **2**.

there is a recent example of ferromagnetically coupled copper centers bridged by a peroxo ligand.⁴⁸ As such, we cannot currently discern between ferro- or antiferromagnetic coupling in **2**.

To further interrogate the solution state structure of **2**, and to probe the assigned oxidation states of Ni, we turned to Ni K-edge X-ray absorption spectroscopy (XAS). The Ni K-edge of **2** (8346.1 eV) occurs at higher energy relative to **1** (8345.4 eV, Figure 3A and Figure S5). The difference in the Ni K-edge between **1** and **2** is outside of error (± 0.4 eV), but it should be noted that one-electron oxidation from Ni^{II} to Ni^{III} in synthetic complexes produces shifts ranging from 0 to 1.8 eV and care must therefore be taken in interpreting this shift as an indicator of oxidation state change.^{49–52} The pre-edge features for **1** and **2** are the same within error. The extended X-ray absorption fine structure (EXAFS) region of **1** can be fit to a model containing three carbon atoms and one chlorine atom in the first shell (Figure S6 and Table S1). Despite poor data quality, analysis of the EXAFS region of **2** suggests a reasonable fit with a simple model containing three carbon atoms and one oxygen atom in the first shell consistent with the structure obtained by SXR (Figure 3B and S7 and Table S2). A poor fit resulted from a model containing a Cl atom,

supporting the loss of this ligand upon reaction with oxygen. Taken together, the observed bond lengths, magnetic properties, and shift in the Ni K-edge of complex **2** support the assignment of a Ni^{III} oxidation state.

We synthesized the ¹⁸O₂ isotopologue of **2** to further characterize the O–O bond through vibrational spectroscopy. However, we have been unable to assign a vibrational band to the O–O stretch by either infrared or Raman spectroscopy of **2** at low temperatures. We attribute the lack of an observable peroxo O–O stretch to either Raman laser photodegradation of **2** or features overlapping with peaks from the BAr^F₄[−] counterion (Figure S8).

With complex **2** in hand, we sought to examine its reactivity, particularly with regard to the possible reversibility of dioxygen binding. Subjecting **2** to several freeze-pump-thaw cycles in DCM resulted in no change in the UV-vis spectrum of the solution. This observation excludes an equilibrium dissociation of O₂. However, addition of 10 equivalents of tetrabutylammonium chloride (TBACl) to **2** in DCM at −78 °C produced a color change from dark purple to green upon warming to −50 °C and 87% recovery of **1** was observed by ¹H NMR spectroscopy (Figure S9, S10). Complex **2** similarly reacts with tetrabutylammonium hydroxide at −50 °C, although the Ni-containing products of this reaction are not well-defined. The balanced reaction with Cl[−] requires the formal release of O₂. However, we have not been able to observe dioxygen release into the headspace by GC analysis. We hypothesize that a short-lived, reactive oxygen species (potentially singlet oxygen or hydrogen peroxide) that reacts further in solution may be generated.⁵³ However, the observed reactivity suggests that if such Ni₂(μ-1,2-peroxo) complexes are generated in oxygen evolution catalysts, O₂ release may be dependent on reaction with nucleophilic species as opposed to direct dissociative O₂ loss.

In summary, we have generated and thoroughly characterized the first example of a bimetallic Ni^{III}₂(μ-1,2-peroxo) complex, **2**. The SXR structure, along with XAS, ¹H NMR and UV-vis spectra of **2** confirm the assignment of a Ni^{III}₂(μ-1,2-peroxo) moiety. Furthermore, this complex is reactive towards nucleophiles such as Cl[−] and OH[−], likely releasing reactive O₂ species. Taken together, these data demonstrate that Ni^{III}₂(μ-1,2-peroxo) species are synthetically accessible and support the hypothesis that related species may be viable intermediates in Ni-based oxygen evolution catalysts.

ASSOCIATED CONTENT

Supporting Information

The Supporting Information is available free of charge online.

AUTHOR INFORMATION

Corresponding Author

jsanderson@uchicago.edu
John S. Anderson

Notes

The authors declare no competing financial interests.

ACKNOWLEDGMENT

Work presented here was funded by the following sources: This work was supported by a 3M NTFA and an NSF CAREER award to JSA: Grant No. 1654144. NZ is supported by the Na-

tional Science Foundation Graduate Research Fellowship under Grant No. DGE-1746045. MRCAT operations are supported by the Department of Energy and the MRCAT member institutions. This research used resources of the Advanced Photon Source, a U.S. Department of Energy (DOE) Office of Science User Facility operated for the DOE Office of Science by Argonne National Laboratory under Contract No. DE-AC02-06CH11357. We thank Dr. Mark Warren, Dr. Joshua Wright and Dr. John Katsoudas for assistance with XAS data acquisition at beamline 10-BM-A,B. We also thank John Hack (UChicago), Ida DiMucci (Cornell) and Prof. Kyle Lancaster (Cornell) for helpful discussions about and assistance with vibrational spectroscopy.

REFERENCES

- (1) Lewis, N. S.; Nocera, D. G. Powering the Planet: Chemical Challenges in Solar Energy Utilization. *Proc. Natl. Acad. Sci. U.S.A.* **2006**, *103*, 15729–15735.
- (2) Singh, A.; Spiccia, L. Water Oxidation Catalysts Based on Abundant 1st Row Transition Metals. *Coord. Chem. Rev.* **2013**, *257*, 2607–2622.
- (3) Hall, D. S.; Lockwood, D. J.; Bock, C.; Macdougall, B. R.; Lockwood, D. J. Nickel Hydroxides and Related Materials: A Review of Their Structures, Synthesis and Properties. *Proc. R. Soc. A* **2014**, *471*, 1–65.
- (4) Burke, M. S.; Enman, L. J.; Batchellor, A. S.; Zou, S.; Boettcher, S. W. Oxygen Evolution Reaction Electrocatalysis on Transition Metal Oxides and (Oxy)Hydroxides: Activity Trends and Design Principles. *Chem. Mater.* **2015**, *27*, 7549–7558.
- (5) Chen, Y.; Rui, K.; Zhu, J.; Dou, S. X.; Sun, W. Recent Progress on Nickel-Based Oxide/(Oxy)Hydroxide Electrocatalysts for the Oxygen Evolution Reaction. *Chem. Eur. J.* **2019**, *25*, 703–713.
- (6) McCrory, C. C. L.; Jung, S.; Peters, J. C.; Jaramillo, T. F. Benchmarking Heterogeneous Electrocatalysts for the Oxygen Evolution Reaction. *J. Am. Chem. Soc.* **2013**, *135*, 16977–16987.
- (7) Hu, M.; Gao, X.; Lei, L.; Sun, Y. Behavior of a Layered Double Hydroxide under High Current Density Charge and Discharge Cycles. *J. Phys. Chem. C* **2009**, *113*, 7448–7455.
- (8) Vialat, P.; Leroux, F.; Mousty, C. Electrochemical Properties of Layered Double Hydroxides Containing 3d Metal Cations. *J. Solid State Electrochem.* **2015**, *19*, 1975–1983.
- (9) Qiu, J.; Villemure, G. Anionic Clay Modified Electrodes: Electrochemical Activity of Nickel(II) Sites in Layered Double Hydroxide Films. *J. Electroanal. Chem.* **1995**, *395*, 159–166.
- (10) Hunter, B. M.; Winkler, J. R.; Gray, H. B. Iron Is the Active Site in Nickel/Iron Water Oxidation Electrocatalysts. *Molecules* **2018**, *23*, 903.
- (11) Li, N.; Bediako, D. K.; Hadt, R. G.; Hayes, D.; Kempa, T. J.; von Cube, F.; Bell, D. C.; Chen, L. X.; Nocera, D. G. Influence of Iron Doping on Tetravalent Nickel Content in Catalytic Oxygen Evolving Films. *Proc. Natl. Acad. Sci. U.S.A.* **2017**, *114*, 1486–1491.
- (12) Corrigan, D. A. The Catalysis of the Oxygen Evolution Reaction by Iron Impurities in Thin Film Nickel Oxide Electrodes. *J. Electrochem. Soc.* **1987**, *134*, 377–384.
- (13) Stevens, M. B.; Trang, C. D. M.; Enman, L. J.; Deng, J.; Boettcher, S. W. Reactive Fe-Sites in Ni/Fe (Oxy)Hydroxide Are Responsible for Exceptional Oxygen Electrocatalysis Activity. *J. Am. Chem. Soc.* **2017**, *139*, 11361–11364.
- (14) Martirez, J. M. P.; Carter, E. A. Unraveling Oxygen Evolution on Iron-Doped β -Nickel Oxyhydroxide: The Key Role of Highly Active Molecular-like Sites. *J. Am. Chem. Soc.* **2019**, *141*, 693–705.
- (15) Enman, L. J.; Burke, M. S.; Batchellor, A. S.; Boettcher, S. W. Effects of Intentionally Incorporated Metal Cations on the Oxygen Evolution Electrocatalytic Activity of Nickel (Oxy)Hydroxide in Alkaline Media. *ACS Catal.* **2016**, *6*, 2416–2423.
- (16) Lee, S.; Banjac, K.; Lingenfelder, M.; Hu, X. Oxygen Isotope Labeling Experiments Reveal Different Reaction Sites for the Oxygen Evolution Reaction on Nickel and Nickel Iron Oxides. *Angew. Chem. Int. Ed.* **2019**, *58*, 10295–10299.
- (17) Lee, S.; Bai, L.; Hu, X. Deciphering Iron-dependent Activity in Oxygen Evolution Catalyzed by Nickel Iron Layered Double Hydroxide. *Angew. Chem. Int. Ed.* **2020**, DOI: 10.1002/anie.201915803.
- (18) McAlpin, J. G.; Surendranath, Y.; Dincă, M.; Stich, T. A.; Stoian, S. A.; Casey, W. H.; Nocera, D. G.; Britt, R. D. EPR Evidence for Co(IV) Species Produced During Water Oxidation at Neutral pH. *J. Am. Chem. Soc.* **2010**, *132*, 6882–6883.
- (19) Zhang, M.; de Respinis, M.; Frei, H. Time-Resolved Observations of Water Oxidation Intermediates on a Cobalt Oxide Nanoparticle Catalyst. *Nat. Chem.* **2014**, *6*, 362–367.
- (20) Camasso, N. M.; Sanford, M. S. Design, Synthesis, and Carbon-Heteroatom Coupling Reactions of Organometallic Nickel(IV) Complexes. *Science* **2015**, *347*, 1218–1220.
- (21) Watson, M. B.; Rath, N. P.; Mirica, L. M. Oxidative C–C Bond Formation Reactivity of Organometallic Ni(II), Ni(III), and Ni(IV) Complexes. *J. Am. Chem. Soc.* **2017**, *139*, 35–38.
- (22) Roberts, C. C.; Chong, E.; Kampf, J. W.; Canty, A. J.; Ariafield, A.; Sanford, M. S. Nickel(II/IV) Manifold Enables Room-Temperature C(Sp³)–H Functionalization. *J. Am. Chem. Soc.* **2019**, *141*, 19513–19520.
- (23) Meucci, E. A.; Ariafield, A.; Canty, A. J.; Kampf, J. W.; Sanford, M. S. Aryl–Fluoride Bond-Forming Reductive Elimination from Nickel(IV) Centers. *J. Am. Chem. Soc.* **2019**, *141*, 13261–13267.
- (24) Nurdin, L.; Spasyuk, D. M.; Fairburn, L.; Piers, W. E.; Maron, L. Oxygen–Oxygen Bond Cleavage and Formation in Co(II)-Mediated Stoichiometric O₂ Reduction via the Potential Intermediacy of a Co(IV) Oxy Radical. *J. Am. Chem. Soc.* **2018**, *140*, 16094–16105.
- (25) Lee, Y.; Park, G. Y.; Lucas, H. R.; Vajda, P. L.; Kamaraj, K.; Vance, M. A.; Milligan, A. E.; Woertink, J. S.; Siegler, M. A.; Narducci Sarjeant, A. A.; Zakharov, L. N.; Rheingold, A. L.; Solomon, E. I.; Karlin, K. D. Copper(I)/O₂ Chemistry with Imidazole Containing Tripodal Tetradentate Ligands Leading to μ -1,2-Peroxo-Dicopper(II) Species. *Inorg. Chem.* **2009**, *48*, 11297–11309.

- (26) Comba, P.; Haaf, C.; Helmle, S.; Karlin, K. D.; Pandian, S.; Waleska, A. Dioxygen Reactivity of New Bispidine-Copper Complexes. *Inorg. Chem.* **2012**, *51*, 2841–2851.
- (27) Fukuzumi, S.; Mandal, S.; Mase, K.; Ohkubo, K.; Park, H.; Benet-Buchholz, J.; Nam, W.; Llobet, A. Catalytic Four-Electron Reduction of O₂ via Rate-Determining Proton-Coupled Electron Transfer to a Dinuclear Cobalt- μ -1,2-Peroxo Complex. *J. Am. Chem. Soc.* **2012**, *134*, 9906–9909.
- (28) Battaini, G.; Casella, L.; Gullotti, M.; Monzani, E.; Nardin, G.; Perotti, A.; Randaccio, L.; Santagostini, L.; Heinemann, F. W.; Schindler, S. Structure and Reactivity Studies on Dinuclear Copper Complexes of the Ligand α , α' -Bis[bis[1-(1'-Methyl-2'-Benzimidazolyl)Methyl]Amino]-m-Xylene. *Eur. J. Inorg. Chem.* **2003**, *2003*, 1197–1205.
- (29) Würtele, C.; Sander, O.; Lutz, V.; Waitz, T.; Tuczek, F.; Schindler, S. Aliphatic C–H Bond Oxidation of Toluene Using Copper Peroxo Complexes That Are Stable at Room Temperature. *J. Am. Chem. Soc.* **2009**, *131*, 7544–7545.
- (30) Ookubo, T.; Sugimoto, H.; Nagayama, T.; Masuda, H.; Sato, T.; Tanaka, K.; Maeda, Y.; Ōkawa, H.; Hayashi, Y.; Uehara, A.; Suzuki, M. Cis- μ -1,2-Peroxo Diiron Complex: Structure and Reversible Oxygenation. *J. Am. Chem. Soc.* **1996**, *118*, 701–702.
- (31) Tanase, T.; Onaka, T.; Nakagoshi, M.; Kinoshita, I.; Shibata, K.; Doe, M.; Fujii, J.; Yano, S. Peroxo-Bridged Dinuclear Cobalt(III) Complexes Containing N-Glycoside Ligands from Tris(2-Aminoethyl)Amine and D-Glucose or Maltose. *Inorg. Chem.* **1999**, *38*, 3150–3159.
- (32) Hikichi, S.; Yoshizawa, M.; Sasakura, Y.; Akita, M.; Moro-Oka, Y. First Synthesis and Structural Characterization of Dinuclear M(III) Bis(μ -Oxo) Complexes of Nickel and Cobalt with Hydrotris(Pyrazolyl)Borate Ligand. *J. Am. Chem. Soc.* **1998**, *120*, 10567–10568.
- (33) Shiren, K.; Ogo, S.; Fujinami, S.; Hayashi, H.; Suzuki, M.; Uehara, A.; Watanabe, Y.; Moro-oka, Y. Synthesis, Structures, and Properties of Bis(μ -oxo)nickel(III) and Bis(μ -superoxo)nickel(II) Complexes: An Unusual Conversion of a Ni^{III}₂(μ -O)₂ Core into a Ni^{II}₂(μ -OO)₂ Core by H₂O₂ and Oxygenation of Ligand. *J. Am. Chem. Soc.* **2000**, *122*, 254–262.
- (34) Morimoto, Y.; Takagi, Y.; Saito, T.; Ohta, T.; Ogura, T.; Tohnai, N.; Nakano, M.; Itoh, S. A Bis(μ -Oxido)Dinickel(III) Complex with a Triplet Ground State. *Angew. Chem. Int. Ed.* **2018**, *57*, 7640–7643.
- (35) Cho, J.; Furutachi, H.; Fujinami, S.; Tosha, T.; Ohtsu, H.; Ikeda, O.; Suzuki, A.; Nomura, M.; Uruga, T.; Tanida, H.; Kawai, T.; Tanaka, K.; Kitagawa, T.; Suzuki, M. Sequential Reaction Intermediates in Aliphatic C–H Bond Functionalization Initiated by a Bis(μ -Oxo)Dinickel(III) Complex. *Inorg. Chem.* **2006**, *45*, 2873–2885.
- (36) Cramer, S. P.; Brunold, T. C.; Mandimutsira, B. S.; Riordan, C. G.; Yamarik, J. L.; Gu, W.; Brunold, T. C.; Gu, W.; Cramer, S. P.; Riordan, C. G. Dioxygen Activation by a Nickel Thioether Complex: Characterization of a Ni^{III}₂(μ -O)₂ Core. *J. Am. Chem. Soc.* **2002**, *123*, 9194–9195.
- (37) Itoh, S.; Bandoh, H.; Nagatomo, S.; Kitagawa, T.; Fukuzumi, S. Aliphatic Hydroxylation by a Bis(μ -Oxo)Dinickel(III) Complex. *J. Am. Chem. Soc.* **1999**, *121*, 8945–8946.
- (38) Honda, K.; Cho, J.; Matsumoto, T.; Roh, J.; Furutachi, H.; Tosha, T.; Kubo, M.; Fujinami, S.; Ogura, T.; Kitagawa, T.; Suzuki, M. Oxidation Reactivity of Bis(μ -Oxo)Dinickel(III) Complexes: Arene Hydroxylation of the Supporting Ligand. *Angew. Chem. Int. Ed.* **2009**, *48*, 3304–3307.
- (39) Kieber-Emmons, M. T.; Schenker, R.; Yap, G. P. A.; Brunold, T. C.; Riordan, C. G. Spectroscopic Elucidation of a Peroxo Ni₂(μ -O₂) Intermediate Derived from a Nickel(I) Complex and Dioxygen. *Angew. Chem. Int. Ed.* **2004**, *43*, 6716–6718.
- (40) Rettenmeier, C. A.; Wadepohl, H.; Gade, L. H. Structural Characterization of a Hydroperoxo Nickel Complex and Its Autoxidation: Mechanism of Interconversion between Peroxo, Superoxo, and Hydroperoxo Species. *Angew. Chem. Int. Ed.* **2015**, *54*, 4880–4884.
- (41) Duan, P.-C.; Manz, D.-H.; Dechert, S.; Demeshko, S.; Meyer, F. Reductive O₂ Binding at a Dihydride Complex Leading to Redox Interconvertible μ -1,2-Peroxo and μ -1,2-Superoxo Dinickel(II) Intermediates. *J. Am. Chem. Soc.* **2018**, *140*, 4929–4939.
- (42) Goetz, M. K.; Hill, E. A.; Filatov, A. S.; Anderson, J. S. Isolation of a Terminal Co(III)-Oxo Complex. *J. Am. Chem. Soc.* **2018**, *140*, 13176–13180.
- (43) Scepianiak, J. J.; Fulton, M. D.; Bontchev, R. P.; Duesler, E. N.; Kirk, M. L.; Smith, J. M. Structural and Spectroscopic Characterization of an Electrophilic Iron Nitrido Complex. *J. Am. Chem. Soc.* **2008**, *130*, 10515–10517.
- (44) Scepianiak, J. J.; Vogel, C. S.; Khusniyarov, M. M.; Heinemann, F. W.; Meyer, K.; Smith, J. M. Synthesis, Structure, and Reactivity of an Iron(V) Nitride. *Science* **2011**, *331*, 1049–1052.
- (45) Hill, E. A.; Zhao, N.; Filatov, A. S.; Anderson, J. S. Nickel(II)-Methyl Complexes Adopting Unusual Seesaw Geometries. *Chem. Commun.* **2020**, DOI: 10.1039/c9cc09249h.
- (46) Holze, P.; Corona, T.; Frank, N.; Braun-Cula, B.; Herwig, C.; Company, A.; Limberg, C. Activation of Dioxygen at a Lewis Acidic Nickel(II) Complex: Characterization of a Metastable Organoperoxide Complex. *Angew. Chem. Int. Ed.* **2017**, *56*, 2307–2311.
- (47) Vaska, L. Dioxygen-Metal Complexes: Toward a Unified View. *Acc. Chem. Res.* **1976**, *9*, 175–183.
- (48) Kindermann, N.; Bill, E.; Dechert, S.; Demeshko, S.; Reiherse, E. J.; Meyer, F. A Ferromagnetically Coupled (S = 1) Peroxodicopper(II) Complex. *Angew. Chem. Int. Ed.* **2015**, *54*, 1738–1743.
- (49) Colpas, G. J.; Maroney, M. J.; Bagyinka, C.; Kumar, M.; Willis, W. S.; Suib, S. L.; Mascharak, P. K.; Baidya, N. X-Ray Spectroscopic Studies of Nickel Complexes, with Application to the Structure of Nickel Sites in Hydrogenases. *Inorg. Chem.* **1991**, *30*, 920–928.
- (50) Mondal, P.; Pirovano, P.; Das, A.; Farquhar, E. R.; McDonald, A. R. Hydrogen Atom Transfer by a High-Valent Nickel-Chloride Complex. *J. Am. Chem. Soc.*

2018, *140*, 1834–1841.

- (51) Corona, T.; Draksharapu, A.; Padamati, S. K.; Gamba, I.; Martin-Diaconescu, V.; Acuña-Parés, F.; Browne, W. R.; Company, A. Rapid Hydrogen and Oxygen Atom Transfer by a High-Valent Nickel–Oxygen Species. *J. Am. Chem. Soc.* **2016**, *138*, 12987–12996.
- (52) Cho, J.; Sarangi, R.; Annaraj, J.; Kim, S. Y.; Kubo, M.; Ogura, T.; Solomon, E. I.; Nam, W. Geometric and Electronic Structure and Reactivity of a Mononuclear Side-on Nickel(III)-Peroxo Complex. *Nat. Chem.* **2009**, *1*, 568–572.
- (53) Greer, A. Christopher Foote's Discovery of the Role of Singlet Oxygen [$^1\text{O}_2$ ($^1\Delta_g$)] in Photosensitized Oxidation Reactions. *Acc. Chem. Res.* **2006**, *39*, 797–804.

Authors are required to submit a graphic entry for the Table of Contents (TOC) that, in conjunction with the manuscript title, should give the reader a representative idea of one of the following: A key structure, reaction, equation, concept, or theorem, etc., that is discussed in the manuscript. Consult the journal's Instructions for Authors for TOC graphic specifications.

